

1 **Short title:** Function of vacuolar iron transporters in wheat

2

3 **Corresponding author:** Janneke Balk, John Innes Centre, Colney Lane, Norwich NR4 7UH, UK;

4 Phone: + 44 1603 450621; E-mail: janneke.balk@jic.ac.uk

5

6 **Title: Vacuolar Iron Transporter TaVIT2 transports Fe and Mn and is**
7 **effective for biofortification**

8

9 **James M. Connorton^{1,2}, Eleanor R. Jones¹, Ildefonso Rodríguez-Ramiro³, Susan**
10 **Fairweather-Tait³, Cristobal Uauy¹ and Janneke Balk^{1,2}**

11

12 ¹ Department of Biological Chemistry, John Innes Centre, Colney Lane, Norwich NR4 7UH, UK

13 ² School of Biological Sciences, University of East Anglia, Norwich, NR4 7TJ, UK

14 ³ Norwich Medical School, University of East Anglia, Norwich, NR4 7UQ, UK

15

16 **One sentence summary:** Altering expression of a vacuolar iron transporter doubles iron content
17 in white wheat flour

18

19 **List of author contributions:** C.U. and J.B. conceived and designed the project; J.M.C. and
20 E.R.J. designed and performed experiments; I.R.R. carried out the bioavailability assays; All
21 authors analysed and interpreted data; J.M.C. and J.B. co-wrote the paper with contributions
22 from the other authors.

23

24 **Key words:** Biofortification, Micronutrient, Iron deficiency anaemia, Wheat, Barley, Endosperm,
25 Metal transport

26

27

28

29 Abstract

30 Increasing the intrinsic nutritional quality of crops, known as biofortification, is viewed as a
31 sustainable approach to alleviate micronutrient deficiencies. In particular iron deficiency
32 anaemia is a major global health issue, but the iron content of staple crops such as wheat is
33 difficult to change because of genetic complexity and homeostasis mechanisms. To identify
34 target genes for biofortification of wheat (*Triticum aestivum*), we functionally characterized
35 homologs of the *Vacuolar Iron Transporter (VIT)*. The wheat genome contains two *VIT* paralogs,
36 *TaVIT1* and *TaVIT2*, which have different expression patterns, but are both low in the
37 endosperm. *TaVIT2*, but not *TaVIT1*, was able to rescue growth of a yeast mutant lacking the
38 vacuolar iron transporter. *TaVIT2* also complemented a manganese transporter mutant, but not
39 a vacuolar zinc transporter mutant. By over-expressing *TaVIT2* under the control of an
40 endosperm-specific promoter, we achieved a > 2-fold increase in iron in white flour fractions,
41 exceeding minimum legal fortification levels in countries such as the UK. The anti-nutrient
42 phytate was not increased and the iron in the white flour fraction was bioavailable in-vitro,
43 suggesting that food products made from the biofortified flour could contribute to improved iron
44 nutrition. The single-gene approach impacted minimally on plant growth and was also effective
45 in barley. Our results show that by enhancing vacuolar iron transport in the endosperm, this
46 essential micronutrient accumulated in this tissue bypassing existing homeostatic mechanisms.
47

48 Introduction

49 Iron is essential for plant growth and needed for a range of cellular processes involving electron
50 transfer or redox-dependent catalysis (Kobayashi and Nishizawa, 2012). However, excess
51 levels of iron are toxic to cells and therefore organisms have evolved tight regulation and
52 storage mechanisms. Plants store iron in ferritin or sequestered in vacuoles, with different
53 species and tissues favouring one storage mechanism over another (Briat et al., 2010). Iron
54 stored in seeds provides for essential iron enzymes during germination before the seedling
55 develops a root and is able to take up iron independently.

56 Iron is also an essential micronutrient for human nutrition, and over a billion people suffer from
57 iron-deficiency anaemia (WHO, 2008). Seeds such as rice, wheat and pulses are a major
58 source of iron, especially in diets that are low in meat. To combat iron deficiency, more than 84
59 countries have legislation for chemical fortification of flours milled from wheat, corn and rice with
60 iron salts or iron powder (www.ffinetwork.org/global_progress/index.php). A more sustainable
61 approach is biofortification, or increasing the intrinsic micronutrient content of crops through
62 traditional breeding or transgenic technology (Vasconcelos et al., 2017).

63 A key gene involved in iron loading in seeds, *VACUOLAR IRON TRANSPORTER1 (VIT1)*, was
64 first identified in Arabidopsis (Kim et al., 2006), as a homolog of yeast *Ca²⁺-SENSITIVE*
65 *CROSS-COMPLEMENTER (CCC1)*, which transports iron into yeast vacuoles (Li et al., 2001)
66 and manganese into Golgi vesicles (Lapinskas et al., 1996). *VIT1* is highly expressed in
67 ripening Arabidopsis seeds, and targets iron to the vacuoles of the endodermis and veins of the

68 embryo (Kim et al., 2006; Roschzttardt et al., 2009). Expression of *VIT1* also increases the
69 manganese content of yeast cells (Kim et al., 2006), and it has a supporting role in manganese
70 transport in *Arabidopsis* embryos (Eroglu et al., 2017). The VITs form a unique transporter
71 family, found in plants, fungi and protists such as the malarial parasite *Plasmodium falciparum*,
72 but they are absent from metazoans (Slavic et al., 2016). VITs in plants share a high degree of
73 sequence similarity and the capacity to transport iron, but their biological functions may differ.
74 For example, *TgVIT1* in tulips is involved in petal colour determination (Momonoi et al., 2009).
75 Due to their roles in iron storage, VITs are potentially good candidates for iron biofortification.
76 Indeed, expression of *VIT1* from *Arabidopsis* controlled by a *PATATIN* promoter enhanced the
77 iron content of cassava tubers 3 – 4-fold (Narayanan et al., 2015). Given the promise for
78 biofortification it is surprising that very few VITs from crop species have been characterized,
79 particularly in cereals. Two *VIT* genes have been identified in rice, *OsVIT1* and *OsVIT2*. The
80 genes showed different expression patterns throughout the plant and in response to iron, but
81 were similar with respect to yeast complementation results. Knockout mutants accumulated
82 more iron in the embryo, but this part of the grain is lost during processing to obtain white rice.
83 The effect of overexpressing the *OsVIT* genes was not tested, and in fact virtually nothing is
84 known about the wider physiological effects of overexpressing *VIT* in plants (Ravet et al., 2009).
85 For biofortification of cereal crops, simply increasing the iron content in grains is unlikely to
86 increase their nutritional quality. Micronutrients are concentrated in the aleurone and seed coat,
87 which are commonly removed in the production of polished rice or white wheat flour. The
88 aleurone is also rich in phytate (myo-inositol-1,2,3,4,5,6-hexakisphosphate), a phosphate
89 storage molecule that is a major inhibitor of iron bioavailability in wholegrain products (Hurrell
90 and Egli, 2010). On the other hand, phytate is low in the endosperm (O'Dell et al., 1972),
91 therefore this tissue should be targeted to increase bioavailable dietary iron in cereal food
92 products. Previous biofortification strategies in wheat include overexpression of ferritin, which
93 increased iron levels 1.6 – 1.8-fold but with large variations per line (Singh et al., 2017).
94 Because ferritin is localized in plastids, iron transport into plastids also needs to be upregulated,
95 and this may be a limiting factor in cereal grains. Elegant NanoSIMS (Nanoscale Secondary Ion
96 Mass Spectrometry) studies showed that iron was concentrated in small vacuoles in the wheat
97 aleurone, colocalising with phosphorus - most likely in the form of phytate, but that some also
98 localized in patches in the endosperm (Moore et al., 2012). Other biofortification strategies have
99 focussed on increasing the mobility of iron through overexpression of nicotianamine synthase
100 genes for the production of chelator molecules to translocate iron(II) and other divalent metals
101 (Singh et al., 2017).

102 Here, we identified and functionally characterized *TaVIT1* and *TaVIT2*, the two *VIT* paralogs
103 found in the genome of bread wheat (*Triticum aestivum*). The *VIT* genes differ in expression
104 patterns and their ability to complement yeast metal transporter mutants. Based on these
105 findings we selected *TaVIT2* for overexpression in the endosperm of wheat and barley, resulting
106 in more than twice as much iron in white flour fractions but little impact on plant growth and

107 grain number. Our results suggest that by drawing iron into vacuoles in the endosperm, existing
108 homeostasis mechanisms can be bypassed for a successful biofortification strategy.

109

110

111 Results

112

113 Wheat has two functionally differentiated *VIT* paralogs

114 The newly sequenced and annotated wheat genome (Clavijo et al., 2017) offers the opportunity
115 to make a complete inventory of putative metal transporters in wheat (Borrill et al., 2014). We
116 found that wheat has two *Vacuolar Iron Transporter* genes (*TaVIT1* and *TaVIT2*) on
117 chromosome groups 2 and 5, respectively. As expected in hexaploid wheat, each *TaVIT* gene is
118 represented by 3 copies (homoeologs) from the A, B and D genomes which share 99% identity
119 at the amino acid level (Table S1, Figure S1). *TaVIT1* and *TaVIT2* have ~87% amino acid
120 identity with their closest rice homolog, *OsVIT1* and *OsVIT2*, respectively. Phylogenetic analysis
121 suggests an early evolutionary divergence of the two *VIT* genes, as there are two distinctly
122 branching clades in the genomes of monocotyledonous species, in contrast to one clade in
123 dicotyledons (Figure 1a). The gene expression profiles of *TaVIT1* and *TaVIT2* were queried
124 across 418 RNA-seq samples (Table S2). All homoeologs of *TaVIT2* were in general more
125 highly expressed than *TaVIT1* homoeologs (Figure 1b). In the grains, *TaVIT1* and *TaVIT2* are
126 both expressed in the aleurone, correlating with high levels of iron in this tissue which is
127 removed from white flours during the milling process. In contrast, expression of *TaVIT1* and
128 *TaVIT2* is very low in the starchy endosperm, the tissue from which white flour is extracted.
129 Taken together, differences in phylogeny and expression pattern suggest that *TaVIT1* and
130 *TaVIT2* may have distinct functions.

131

132 *TaVIT2* facilitates transport of iron and manganese

133 To test if the *TaVIT* proteins transport iron, the 2BL *TaVIT1* homoeolog and 5DL *TaVIT2*
134 homoeolog, hereafter referred to as *TaVIT1* and *TaVIT2* respectively, were selected and
135 expressed in yeast lacking the vacuolar iron transporter *Ccc1*. The $\Delta ccc1$ yeast strain is
136 sensitive to high concentrations of iron in the medium because of its inability to store iron in the
137 vacuole. *TaVIT2* fully rescued growth of $\Delta ccc1$ yeast exposed to a high concentration of FeSO_4 ,
138 but *TaVIT1* was no different from the empty vector control (Figure 2a). Yeast *Ccc1* can transport
139 both iron and manganese (Lapinskas et al., 1996). Therefore, we carried out yeast
140 complementation using the $\Delta pmr1$ mutant, which is unable to transport manganese into Golgi
141 vesicles and cannot grow in the presence of toxic levels of this metal (Lapinskas et al., 1995).
142 We found that expression of *TaVIT2* in $\Delta pmr1$ yeast partially rescued the growth impairment on
143 high concentrations of MnCl_2 , indicating that *TaVIT2* can transport manganese (Figure 2b). We
144 also tested if *TaVIT1* and *TaVIT2* are able to rescue growth of the yeast $\Delta zrc1$ strain, which is
145 defective in vacuolar zinc transport, but neither *TaVIT* gene was able to rescue growth on high
146 zinc concentrations (Figure 2c).

147 Western blot analysis showed that both proteins were produced in yeast, but that *TaVIT1* and
148 *TaVIT2* might differ in their intracellular distribution (Figure 2d). *TaVIT2* was abundant in
149 vacuolar membranes, co-fractionating with the vacuolar marker protein *Vph1*. *TaVIT1* was also

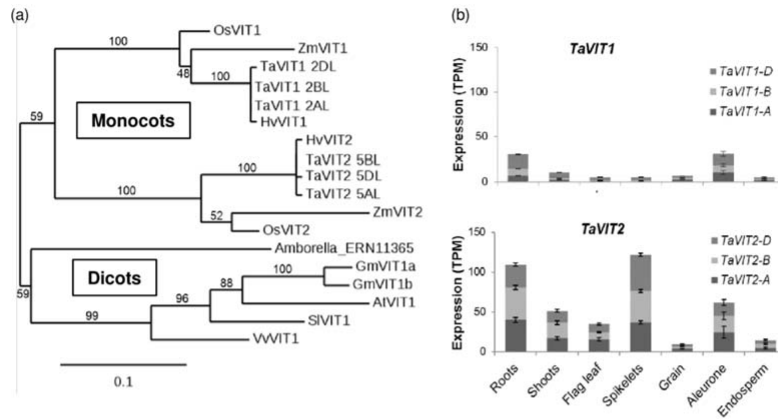


Figure 1 The wheat genome encodes two *VIT* paralogs with different expression patterns. (a) Phylogenetic tree of *VIT* genes from selected plant species: *At*, *Arabidopsis thaliana*; *Gm*, *Glycine max* (soybean); *Hv*, *Hordeum vulgare* (barley); *Os*, *Oryza sativa* (rice); *Sl*, *Solanum lycopersicum* (potato); *Ta*, *Triticum aestivum* (wheat); *Vv*, *Vitis vinifera* (grape); *Zm*, *Zea mays* (maize). Numbers above or below branches represent bootstrapping values for 100 replications. (b) Gene expression profiles of *TaVIT1* and *TaVIT2* homoeologs using RNA-seq data from expVIP. Bars indicate mean transcripts per million (TPM) \pm SEM, full details and metadata in Table S2.

150 found in the vacuolar membrane fraction, but based on higher abundance in the total fraction, it
 151 appeared that most of the TaVIT1 protein was targeted to other membranes. Closer inspection
 152 of the amino acid sequences revealed that TaVIT2 contains a universally conserved dileucine
 153 motif for targeting to the vacuolar membrane (Bonifacino and Traub, 2003; Wang et al., 2014),
 154 which is absent from TaVIT1 (Figure S1b). Therefore, TaVIT1 may be able to transport iron, but
 155 will not complement $\Delta ccc1$ yeast. Instead, we tested if TaVIT1 was able to complement the

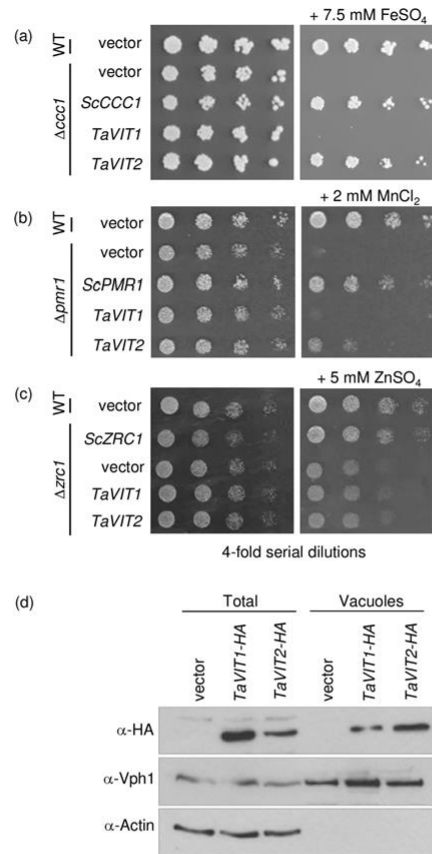


Figure 2 TaVIT2 facilitates iron and manganese transport. (a,b,c) Yeast complementation assays of *TaVIT1* and *TaVIT2* in $\Delta ccc1$ (a), $\Delta pmr1$ (b) and $\Delta zrc1$ (c) compared to yeast that is wild type (WT) for these three genes. The yeast (Sc) *CCC1*, *PMR1* and *ZRC1* genes were used as positive controls. Cells were spotted in a 4-fold dilution series and grown for 2-3 days on plates \pm 7.5 mM FeSO₄ ($\Delta ccc1$), 2 mM MnCl₂ ($\Delta pmr1$) or 5 mM ZnSO₄ ($\Delta zrc1$). (d) Immunoblots of total and vacuolar protein fractions from yeast cells expressing haemagglutinin (HA)-tagged *TaVIT1* or *TaVIT2*. The HA-tag did not inhibit the function of *TaVIT2* as it was able to complement $\Delta ccc1$ yeast (data not shown). Vhp1 was used as a vacuolar marker and the absence of actin shows the purity of the vacuolar fraction.

156 $\Delta fet3$ yeast mutant, which is defective in high-affinity iron transport across the plasma
 157 membrane. $\Delta fet3$ mutants cannot grow on medium depleted of iron with the chelator BPS, but
 158 expression of *TaVIT1* rescued growth under these conditions (Figure S2). These data indicate
 159 that both *TaVIT1* and *TaVIT2* are able to transport iron, but that their localization in the cell may
 160 differ.
 161

162 Over-expression of *TaVIT2* in the endosperm of wheat specifically increased the iron
163 concentration in white flour

164 The functional characterization of *TaVIT1* and *TaVIT2* suggested that *TaVIT2*, as a *bona fide*
165 iron transporter localized to vacuoles, is a good candidate for iron biofortification. We placed the
166 *TaVIT2* gene under the control of the wheat endosperm-specific promoter of the *High Molecular*
167 *Weight Glutenin-D1 (HMW)* gene (Lamacchia et al., 2001) and transformed the construct
168 together with a hygromycin resistance marker into the wheat cultivar 'Fielder' (Figure 3a). A total
169 of 27 hygromycin-resistant plants were isolated and the copy number of the transgene was
170 determined by qPCR. There were ten lines with a single copy insertion, and the highest number
171 of insertions was 30. The transgene copy number correlated well with expression of *TaVIT2* in
172 the developing grain ($R^2 = 0.60$, $p < 0.01$, Figure 3b; Figure S3). *TaVIT2* expression was
173 increased 3.8 ± 0.2 -fold in single copy lines and more than 20-fold in lines with multiple
174 transgenes compared to non-transformed controls.

175 Mature wheat grains from transgenic lines and non-transformed controls were dissected with a
176 platinum-coated blade and stained for iron using Perls' Prussian Blue. In non-transformed
177 controls, positive blue staining was visible in the embryo, scutellum and aleurone layer, but the
178 endosperm contained little iron (Figure 4). In lines over-expressing *TaVIT2* the Perls' Prussian
179 Blue staining was visibly increased, in particular around the groove and in patches of the
180 endosperm. To quantify the amount of iron, grains from individual lines were milled to produce
181 wholemeal flour, which was sieved to obtain a white flour fraction, followed by element analysis
182 using Inductively Coupled Plasma-Optical Emission Spectroscopy (ICP-OES) (Figure 5a, Table
183 S3). Iron levels were consistently enhanced 2-fold in white flour, from $9.7 \pm 0.3 \mu\text{g/g}$ in control
184 lines to $21.7 \pm 2.7 \mu\text{g/g}$ in lines with a single copy of *HMW-TaVIT2* ($p < 0.05$). Additional
185 transgene copies resulted in a similar 2-fold increase in iron, whereas lines with ≥ 20 copies
186 contained 4-fold more iron than controls, to $41.5 \pm 8.2 \mu\text{g/g}$ in white flour ($p < 0.05$). The iron
187 content of wholemeal flour of single insertion lines was similar to control lines, but increased up
188 to 2-fold in high copy lines ($p < 0.01$). No statistically significant differences were found for other
189 metals in single-copy *HMW-TaVIT2* wheat grains, such as zinc, manganese and magnesium
190 (Table S3), nor for the heavy metal contaminants cadmium and lead (Table S4). In lines with
191 ≥ 20 copies of *HMW-TaVIT2* significant increases in all elements except Mn and Pb were seen
192 ($p < 0.05$), presumably as a secondary effect.

193

194 White flour has an improved iron:phytate ratio and the iron is bioavailable

195 Because the high phytate content of cereal grains inhibits bioavailability of minerals, we
196 measured phytate levels in *TaVIT2* over-expressing lines, but found no significant increase in
197 phytate in white flour (Figure 5b), although there was a slight increase in phosphorus (Table
198 S3). There was also a small increase in phytate in wholemeal flour produced from those lines.
199 Considering the 2-fold increase in iron, the iron:phytate molar ratio was improved 2-fold in white
200 flour of *HMW-TaVIT2* lines, but unaffected in wholemeal flour (Figure 5c).

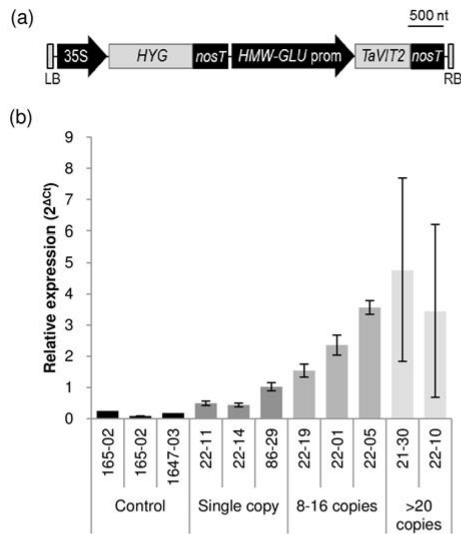


Figure 3 Expression of *TaVIT2* in cisgenic lines. (a) Diagram of the transfer-DNA construct: LB, left border; 35S, CaMV 35S promoter; *HYG*, hygromycin resistance gene; *nosT*, *nos* terminator; *HMW-GLU* prom, high molecular weight glutenin-D1-1 promoter; *TaVIT2*, wheat *VIT2-D* gene; RB, right border. (b) Relative expression levels of *TaVIT2* in developing grains at 10 days post anthesis as determined by quantitative real-time PCR and normalized to housekeeping gene *Traes_4AL_8CEA69D2F*. Plant identification numbers and copy number of the *HMW-TaVIT2* gene are given below the bars. Bars indicate the mean \pm SEM of 3 independent biological replicates.

201 To investigate the potential bioavailability of the iron, flour samples were subjected to simulated
 202 gastrointestinal digestion and the digests applied to Caco-2 cells, a widely used cellular model
 203 of the small intestine (Glahn et al., 1998). For the purpose of this experiment, the availability of
 204 iron was maximized by treating the samples with phytase and by exposing the cells directly to
 205 the digestate after heat-inactivation of the lytic enzymes. The increase in ferritin protein in Caco-
 206 2 cells after exposure to the digestate was used as a surrogate measure of iron availability. Iron

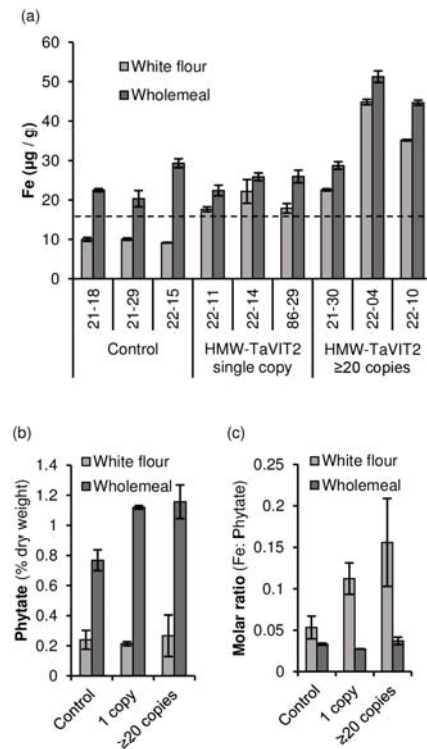


Figure 5 Iron and phytate content of flour milled from *HMW-TaVIT2* wheat lines. (a) Iron concentrations in white and wholemeal flour from 3 control and 6 *HMW-TaVIT2* lines. Bars represent the mean of 2 technical replicates and the deviation of the mean. White flour from *HMW-TaVIT2* lines has significantly more iron than control lines ($n = 3-4$, $p < 0.05$; see Table S3 for all data). The dotted line at 16.5 µg/g iron indicates the minimum requirement for wheat flour milled in the UK. (b) Phytate content of white and wholemeal flour of control and *HMW-TaVIT2* expressing wheat. Bars represent the mean of 2 biological replicates \pm deviation of the mean. (c) Molar ratio of iron:phytate in control and *HMW-TaVIT2* expressing lines. Bars represent the mean of 2 biological replicates and the deviation of the mean.

207 from white flour was taken up by the Caco-2 cells, and more ferritin production was observed
 208 cells exposed to samples from *TaVIT2*-overexpressing lines, however the values were variable
 209 between wheat lines (Figure S4). In contrast, the iron in wholemeal flour, although twice as high
 210 as in white flour, was not available for uptake, as previously noted (Eagling et al., 2014). Further
 211 analysis of breads baked from these flours is necessary to confirm overexpression improves

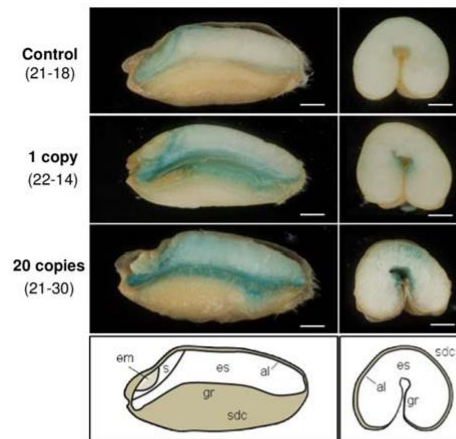


Figure 4 Perl's Prussian Blue staining for iron in grains transformed with *HMW-TaVIT2*. Grains from T_0 wheat plants were dissected longitudinally (left) or transversely (right). em, embryo; s, scutellum; sdc, seed coat; es, endosperm; al, aleurone, gr, groove. The transgene copy number and line number are indicated on the far left. Scale bars = 1 mm.

212 iron bioavailability. These data suggest that relocating iron into the endosperm may be more
 213 effective than increasing total iron in the grain as a biofortification strategy.

214

215 The high-iron phenotype has little impact on plant growth and is maintained in T_2 grains

216 To investigate if *TaVIT2* over-expression affected plant growth, we measured plant height, tiller
 217 number, grain size, number of grains per plant and thousand-grain weight in *TaVIT2* over-

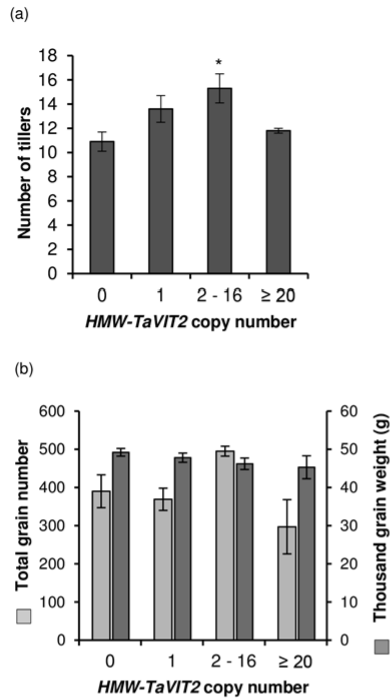


Figure 6 Growth parameters of *HMW-TaVIT2* wheat. (a) Number of tillers and (b) seed output of T_0 wheat plants with indicated *HMW-TaVIT2* copy numbers. Bars indicate mean \pm SEM of the following numbers of biological replicates: zero gene copies, n = 9; 1 gene copy, n = 10; 2 -16 gene copies, n = 9; ≥ 20 gene copies, n = 6. Further details given in Table S5. Asterisk indicates significant difference from negative control (One-way ANOVA with Tukey post-hoc test, * $p < 0.05$).

218 expressing lines and controls. None of these growth parameters were negatively affected by the
 219 *HMW-TaVIT2* transgene in the T_0 generation grown in controlled environment rooms (Figure 6
 220 and Table S5). Conversely, a statistically significant increase in tiller number was seen in plants
 221 containing 2 – 16 copies of the *HMW-TaVIT2* transgene, to 15.3 ± 1.2 compared to the control
 222 of 10.9 ± 0.8 ($p < 0.05$, ANOVA, Table S5). Analysis of further generations and field trials are
 223 required to confirm this effect and its potential impact on yield.

224 Seed from the first T₀ transformant obtained (line 27-02, containing 2 copies of *HMW-TaVIT2*)
225 was planted in a greenhouse to investigate the high-iron trait in the next generation (T₁). The
226 *HMW-TaVIT2* transgene segregated in a 3:1 ratio ($\chi^2=0.29$). Growth of plants in the greenhouse
227 was very different from controlled environmental chambers, but there were no significant
228 differences in growth and yield component traits for *HMW-TaVIT2* plants compared to wild-type
229 segregants or non-transformed controls (Table S6). The iron levels were overall higher in grain
230 from greenhouse-grown plants, even so T₂ grain contained a 2-fold increase in iron in the white
231 flour fraction ($p < 0.05$, Table S6). Taken together, endosperm-specific over-expression of
232 *TaVIT2* has no major growth defects and the iron increase showed a similar trend in the next
233 generation despite different growth conditions.

234

235 **Expression of *HMW-TaVIT2* in barley increases grain iron and manganese content**

236 We also transformed barley (*Hordeum vulgare* cv. Golden Promise) with the *HMW-TaVIT2*
237 construct. The 12 transgenic plants had either 1 or 2 copies of the transgene and were
238 indistinguishable from non-transformed controls with regards to vegetative growth and grain
239 development. Staining with Perls' Prussian Blue showed that, similarly to wheat, there was
240 more iron in transformed grains than controls, and this tended to accumulate in the sub-
241 aleurone region of the endosperm. To quantify the iron and other metals, lines B2 (1 copy) and
242 B3 (2 copies) were selected for ICP-OES analysis and found to contain 2-fold more iron than
243 the control in both white and wholemeal flour (Figure 7). The white flour produced from
244 barley contained relatively high levels of phosphorus, suggesting that there was some aleurone
245 present, so the differences in minerals between white and wholemeal flours are not as
246 pronounced as in wheat. Interestingly, in barley there was also a 2-fold increase in manganese
247 levels (Figure 7). These results indicate that the ability of *TaVIT* to transport manganese, as
248 observed in yeast (Figure 2b), can be operational in plant tissue. Overall, our results indicate
249 that endosperm-specific over-expression of *TaVIT2* is a successful strategy for increasing the
250 iron content in different cereal crop species.

251

252

253

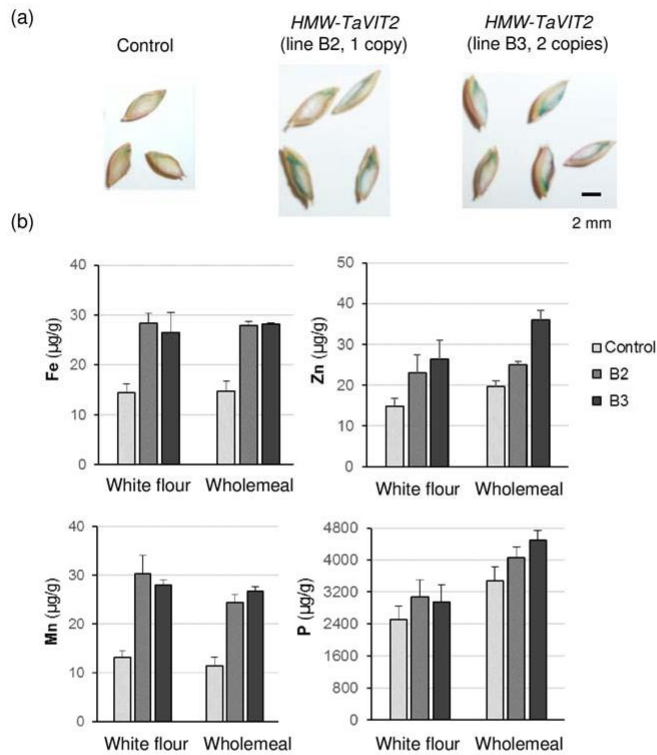


Figure 7 Endosperm-specific over-expression of *TaVIT2* in barley. The *TaVIT2-5DL* gene from wheat under the control of the wheat *HMW-GLU-1D-1* promoter (see Figure 3a for full details) was transformed into barley (*Hordeum vulgare* var. Golden Promise). Positive transformants were selected by hygromycin. (a) Mature barley T_1 grains of a control plant and two transgenic lines stained with Perls' Prussian blue staining for iron. (b) Element analysis in white and wholemeal flours from a control and two *HMW-TaVIT2* over-expressing barley plants. The values are the mean of 2 technical replicates. Error bars represent the deviation of the mean.

254 Discussion

255

256 The recently sequenced wheat genome greatly facilitates gene discovery in this economically
 257 important but genetically complex crop species. In a previous analysis (Borrill et al., 2014) we
 258 identified over 60 putative metal transporters, and started with the functional characterization of
 259 VITs. We selected *TaVIT1-B* and *TaVIT2-D* for our studies. Each *TaVIT* gene has three

260 homoeologs but these share 99% amino acid identity, and those amino acids that differ are not
261 conserved, therefore we believe that our results are representative for all three homoeologs.
262 While TaVIT1 and TaVIT2 are ~87% identical with OsVIT1 and OsVIT2, we found remarkable
263 differences. Each rice VIT has the dileucine motif involved in vacuolar targeting and GFP fusion
264 proteins showed vacuolar localisation when transiently expressed in Arabidopsis protoplasts
265 (Zhang et al., 2012). In wheat, only TaVIT2 has the dileucine motif and this correlated with
266 vacuolar localization of TaVIT2 in yeast. Another striking difference between rice and wheat
267 VITs is the yeast complementation results. *OsVIT1* and *OsVIT2* partially complemented mutants
268 in iron transport ($\Delta ccc1$) and zinc transport ($\Delta zrc1$). In wheat, only *TaVIT2* showed
269 complementation of $\Delta ccc1$ and we saw no evidence of Zn transport, similar to the metal
270 specificity of the yeast homolog. The growth defect of $\Delta ccc1$ was completely rescued by
271 *TaVIT2*, indicating efficient iron transport in contrast to only weak complementation by the rice
272 VIT genes. The production of the rice VIT proteins in yeast was unfortunately not verified by
273 Western blot analysis (Zhang et al., 2012). Our initial experiments showed that wheat *TaVIT1*
274 was poorly expressed in yeast, so the sequence was codon-optimized to remove codons that
275 are rare in *Saccharomyces cerevisiae* (Figure S5). This greatly improved expression of *TaVIT1*
276 to even higher levels than *TaVIT2*, but *TaVIT1* still did not complement the yeast mutants in Fe,
277 Zn or Mn transport. *TaVIT1*, however, did complement the $\Delta fet3$ yeast mutant (Figure S2).
278 Yeast *FET3* is part of a complex directing high-affinity Fe transport across the plasma
279 membrane (Askwith et al., 1994). This suggests that TaVIT1 is indeed a functioning iron
280 transporter but that it mainly localizes to a membrane other than the tonoplast. It will be
281 interesting to identify the amino acid residues that determine metal specificity and/or localization
282 in the VIT family. However, currently there is no crystal structure of any of the VIT family
283 members and no other good structural homology models. Recently, a first glimpse into the
284 transport mechanism was provided, showing that Plasmodium VIT1 is a H⁺ antiporter with
285 strong selectivity for Fe²⁺ (Slavic et al., 2016; Labarbuta et al., 2017).
286

287 Over-expression of the vacuolar iron transporter *TaVIT2* in wheat endosperm was very effective
288 in raising the iron concentration in this tissue. We hypothesize that increased sequestration of
289 iron in the vacuoles creates a sink which then upregulates the relocation of iron to that tissue. If
290 the tissue normally stores iron in vacuoles rather than in ferritin, proteins and chelating
291 molecules for iron mobilisation into the vacuole will already be present. For a sink-driven
292 strategy, timely expression of the gene in a specific tissue is essential: if the protein is produced
293 constitutively, for example using the CaMV 35S promoter, then it will draw iron into all tissues,
294 not in one particular tissue. Interestingly, knock-out mutants of *VIT1* and *VIT2* in rice
295 accumulated more iron in the embryo (Zhang et al., 2012). A likely scenario is that iron
296 distributed to the developing rice grain cannot enter the vacuoles in the aleurone (Kyriacou et
297 al., 2014), and is thus diverted to the embryo. The finding further supports the idea that VITs
298 play a key role in iron distribution in cereal grains. An additional advantage of endosperm-

299 specific expression is that possible growth defects in vegetative tissues are likely to be avoided,
300 as found in our studies.

301

302 Wheat and barley transformed with the same *HMW-TaVIT2* construct showed surprising
303 differences in the accumulation of iron and manganese. Wheat had a 2-fold increase in iron in
304 the endosperm only, whereas barley contained 2-fold more iron in whole grains. Barley grains
305 also contained 2-fold more manganese, but this element was not increased in wheat, even
306 though *TaVIT2* was found to transport both iron and manganese in yeast complementation
307 assays. It is possible that the wheat *HMW* promoter has a different expression pattern in barley.
308 If the promoter is activated in the aleurone cells in addition to the endosperm, this may lead to
309 the observed higher iron concentrations in whole barley grains. The pattern of promoter activity
310 can be further investigated with reporter constructs or by in-situ hybridization specific for the
311 transgene. It is also possible that wheat and barley differ in iron and manganese transport
312 efficiency from roots to shoots, thus affecting the total amount of iron and manganese that is
313 (re)mobilized to the grain.

314

315 In the Americas, Africa and Asia, iron fortification of flours ranges from 30 to 44 µg/g. In Europe,
316 only the UK has a legal requirement for fortification: white and brown flours must contain at least
317 16.5 µg/g iron. We have now achieved this iron concentration in white flour produced from the
318 single-copy *HMW-TaVIT2* lines described here. More copies of *TaVIT2* increased iron levels
319 further, but resulted in accumulation of other metals. Moreover, with ≥ 20 transgene copies
320 there were fewer grains per plant. Combining endosperm-specific *TaVIT2* overexpression with
321 constitutive *NAS* over-expression may be one suitable approach to increase grain iron levels
322 further. A combination strategy using over-expression of *NAS2* and soybean ferritin increased
323 iron levels in polished rice more than 6-fold, from 2 µg/g to 15 µg/g in the field (Trijatmiko et al.,
324 2016). However, combining *NAS* and *FER* over-expression in wheat did not show a synergistic
325 effect: constitutive expression of the rice *NAS2* gene resulted in 2.1-fold more iron in grains and
326 2.5-fold more iron in white flour, but coupled with endosperm-specific expression of *FER*, grain
327 iron content was only 1.6 - 1.8-fold increased, similar to *FER* alone (Singh et al., 2017). As
328 noted before, iron in wheat is mostly stored in vacuoles rather than ferritin, so increasing iron
329 transport into vacuoles combined with increasing iron mobility is likely to be more effective.
330 Nicotianamine is also reported to improve the bioavailability of iron (Zheng et al., 2010), which is
331 a major determinant for the success of any biofortification strategy.

332 On a societal level, a major question is whether wheat biofortified using modern genetic
333 techniques will be accepted by consumers. Our strategy used wheat genetic material (promoter
334 and coding sequence), and could therefore be considered cisgenic. The *HMW-TaVIT2* lines
335 also contain DNA from species other than wheat, such as a hygromycin resistance gene of
336 bacterial origin, but these regions can be removed using CRISPR technology, leaving only
337 wheat DNA. In addition, the wheat lines described here are valuable tools to identify processes

338 regulating iron content of the grain. Identification of the transcription factors that control *VIT*
339 expression would be helpful, but none have been identified so far in any plant species. Once
340 more genetic components of the iron loading mechanism into cereals have been identified,
341 these can be targets of non-transgenic approaches such as TILLING (Krasileva et al., 2017).

342

343

344 **Experimental procedures**

345

346 **Identification of wheat *VIT* genes, phylogenetic analysis and analysis of RNA-seq data**

347 The coding sequences of the wheat *VIT* genes were found by a BLAST search of the rice
348 *OsVIT1* (*LOC_Os09g23300*) and *OsVIT2* (*LOC_Os04g38940*) sequences in Ensembl Plants
349 (<http://plants.ensembl.org>). Full details of the wheat genes are given in Table S1. Sequences of
350 *VIT* genes from other species were found by a BLAST search of the Arabidopsis *AtVIT1*
351 (*AT2G01770*) and rice *VIT* sequences against the Ensembl Plants database. Amino acid
352 alignments were performed using Clustal Omega (<http://www.ebi.ac.uk/Tools/msa/clustalo/>).
353 The tree was plotted with BioNJ with the Jones-Taylor-Thornton matrix and rendered using
354 TreeDyn 198.3. RNA-seq data was obtained from the expVIP database (Borrill et al., 2016;
355 <http://www.wheat-expression.com>). Full details of the data-sets used are given in Table S2.

356

357 **Yeast complementation**

358 Coding DNA sequences for the wheat 2BL *VIT1* homoeolog
359 (TRIAE_CS42_2BL_TGACv1_129586_AA0389520) and the 5DL *VIT2* homoeolog
360 (TRIAE_CS42_5DL_TGACv1_433496_AA1414720) were synthesized and inserted into pUC57
361 vectors by Genscript (Piscataway, NJ, USA). The wheat *VIT* genes were first synthesized with
362 wheat codon usage, but *TaVIT1* was poorly translated in yeast so was re-synthesized with
363 yeast codon usage including a 3x haemagglutinin (HA) tag at the C-terminal end. Untagged
364 codon-optimized *TaVIT1* was amplified from this construct using primers *TaVIT1co-XbaI-F* and
365 *TaVIT1co-EcoRI-R* (see Table S7 for primer sequences). *TaVIT2-HA* was cloned by amplifying
366 the codon sequence without stop codon using primers *TaVIT2-BamHI-F* and *TaVIT2(ns)-EcoRI-*
367 *R*, and by amplifying the HA tag using primers *HAT-EcoRI-F* and *HAT(Stop)-ClaI-R*. The two
368 DNA fragments were inserted into plasmid p416 behind the yeast *MET25* promoter (Mumberg
369 et al., 1995).

370 Genes *ScCCC1*, *ScFET3*, *ScPMR1* and *ScZRC1* were cloned from yeast genomic DNA, using
371 the primer pairs *ScCCC1-BamHI-F* and *ScCCC1-EcoRI-R*, *ScFET3-XbaI-F* and *ScFET3-XhoI-*
372 *R*, *ScPMR1-SpeI-F* and *ScPMR1-XhoI-R*, and *ScZRC1-XbaI-F* and *ScZRC1-EcoRI-R*,
373 respectively. Following restriction digests the DNA fragments were ligated into vector p416-
374 *MET25* and confirmed by sequencing. All constructs were checked by DNA sequencing.

375 The *Saccharomyces cerevisiae* strain BY4741 (MATa *his3Δ1 leu2Δ0 met15Δ0 ura3Δ0*) was
376 used in all yeast experiments. Either wild-type (WT), $\Delta ccc1$ (Li et al., 2001), $\Delta zrc1$ (MacDiarmid

377 et al., 2003), $\Delta pmr1$ (Lapinskas et al., 1995) or $\Delta fet3$ (Askwith et al., 1994) was transformed
378 with approximately 100 ng DNA using the PEG/lithium acetate method (Ito et al., 1983).
379 Complementation analysis was performed via drop assays using overnight cultures of yeast
380 grown in selective synthetic dextrose (SD) media, diluted to approximately 1×10^6 cells/ml,
381 spotted in successive 4 x dilutions onto SD plates containing appropriate supplements. Plates
382 were incubated for 3 days at 30°C. Total yeast protein extraction was performed by alkaline
383 lysis of overnight cultures (Kushnirov, 2000).

384

385 **Preparation of vacuoles from yeast**

386 Preparation of yeast vacuoles was performed using cell fractionation over a sucrose gradient
387 (Hwang et al., 2000; Nakanishi et al., 2001). Briefly, 1 L yeast was grown in selective SD media
388 to an OD_{600} of 1.5-2.0 then centrifuged at 4000 g for 10 min, washed in buffer 1 (0.1 M Tris-HCl
389 pH 9.4, 50 mM β -mercaptoethanol, 0.1 M glucose) and resuspended in buffer 2 (0.9 M sorbitol,
390 0.1 M glucose, 50 mM Tris- 2-(N-morpholino)ethanesulfonic acid (MES) pH 7.6, 5 mM
391 dithiothreitol (DTT), 0.5 x SD media). Zymolyase 20T (Seikagaku, Tokyo, Japan) was added at
392 a concentration of 0.05% (w/v) and cells were incubated for 2 h at 30°C with gentle shaking.
393 After cell wall digestion, spheroplasts were centrifuged at 3000 g for 10 min and then washed in
394 1 M sorbitol before being resuspended in buffer 3 (40 mM Tris-MES, pH 7.6, 1.1 M glycerol,
395 1.5% (w/v) polyvinylpyrrolidone 40,000; 5 mM EGTA, 1 mM DTT, 0.2% (w/v) bovine serum
396 albumin (BSA), 1 mM phenylmethylsulfonyl fluoride (PMSF), 1 x protease inhibitor cocktail
397 (Promega)) and homogenized on ice using a glass homogenizer. The homogenate was
398 centrifuged at 2000 g for 10 min at 4°C and the supernatant was transferred to fresh tubes,
399 while the pellet was resuspended in fresh buffer 3 and centrifuged again. The supernatants
400 were pooled and centrifuged at 150,000 g for 45 min at 4°C to pellet microsomal membranes.
401 For preparation of vacuole-enriched vesicles the pellet was resuspended in 15% (w/w) sucrose
402 in buffer 4 (10 mM Tris-MES pH7.6, 1 mM EGTA, 2 mM DTT, 25 mM KCl, 1.1 M glycerol, 0.2%
403 (w/v) BSA, 1 mM PMSF, 1 x protease inhibitor cocktail) and this was layered onto an equal
404 volume of 35% (w/w) sucrose solution in buffer 4 before centrifugation at 150,000 g for 2 h at
405 4°C. Vesicles were collected from the interface and diluted in buffer 5 (5 mM Tris-MES pH 7.6,
406 0.3 M sorbitol, 1 mM DTT, 1 mM EGTA, 0.1 M KCl, 5 mM $MgCl_2$, 1 mM PMSF, 1 x protease
407 inhibitor cocktail). The membranes were centrifuged at 150,000 g for 45 min at 4°C and
408 resuspended in a minimal volume of buffer 6 (5 mM Tris-MES pH 7.6, 0.3 M sorbitol, 1 mM
409 DTT, 1 mM PMSF, 1 x protease inhibitor cocktail). Vesicles were snap-frozen in liquid nitrogen
410 and stored at -80°C.

411

412 **Generation of transgenic plantlines**

413 The *TaVIT2* gene was amplified using primers *TaVIT2-NcoIF* and *TaVIT2-SpeIR* and cloned
414 into vector pRRes14_RR.301 containing the promoter sequence comprising nucleotides -1187
415 to -3 with respect to the ATG start codon of the *GLU-1D-1* gene, which encodes the high-

416 molecular-weight glutenin subunit 1Dx5 (Lamacchia et al., 2001). The promoter-gene fragment
417 was then cloned into vector pBract202 containing a hygromycin resistance gene and LB and RB
418 elements for insertion into the plant genome (Smedley and Harwood, 2015). The construct was
419 checked by DNA sequencing. Transformation into wheat (cultivar Fielder) and barley (cultivar
420 Golden Promise) were performed by the BRAC T platform at the John Innes Centre using
421 *Agrobacterium*-mediated techniques as described previously (Wu et al., 2003; Harwood et al.,
422 2009). Transgene insertion and copy number in T₀ plants were assessed by iDNA Genetics
423 (Norwich, UK) using qPCR with a Taqman probe. For the T₁ generation, the presence of the
424 hygromycin resistance gene was analysed by PCR with primers Hyg-F and Hyg-R.

425

426 **Plant growth and quantitative analysis**

427 The first generation of transgenic plants (T₀) were grown in a controlled environment room
428 under 16 h light (300 μmol m⁻² s⁻¹) at 18°C / 8 h dark at 15°C with 65% relative humidity. The
429 next generation (T₁) were grown in a glasshouse kept at approximately 20°C with 16 h light.
430 Wheat and barley plants were grown on a mix of 40% medium grade peat, 40% sterilized soil
431 and 20% horticultural grit, and fertilized with 1.3 kg/m³ PG Mix 14+16+18 (Yara UK Ltd,
432 Grimsby, UK) containing 0.09% Fe, 0.16% Mn and 0.04% Zn. Ears from wheat and barley
433 plants were threshed by hand and grain morphometric characteristics, mass and number were
434 determined using a MARVIN universal grain analyser (GTA Sensorik, GmbH, Neubrandenburg,
435 Germany).

436

437 **RNA extraction and qRT-PCR**

438 Samples of developing grain were taken at 10 days post anthesis and frozen in liquid nitrogen.
439 RNA extraction was performed using phenol/chloroform extraction (Box et al., 2011).
440 Developing grains were ground with a pestle and mortar under liquid nitrogen and mixed with
441 RNA extraction buffer (0.1 M Tris-HCl, pH 8; 5 mM EDTA; 0.1 M NaCl, 0.5% (w/v) SDS, 1%
442 (v/v) 2-mercaptoethanol) and Ambion Plant RNA Isolation Aid (ThermoFisher). Samples were
443 centrifuged for 10 min at 15,000 g and the supernatant was added to 1:1 acidic phenol (pH
444 4.3):chloroform. After mixing and incubation at room temperature for 10 min, the upper phase
445 was added to isopropanol containing 0.3 M sodium acetate. Samples were incubated at -80°C
446 for 15 min and centrifuged for 30 min at 15,000 g at 4°C. The supernatant was discarded and
447 the pellet was washed twice in 70% (v/v) ethanol and dried, before being resuspended in
448 RNase-free water. RNA was DNase treated using TURBO DNase-free kit (ThermoFisher) as
449 per manufacturer's instructions, DNase inactivation reagent was added and the samples were
450 centrifuged at 10,000 g for 90 s. Supernatant containing RNA was retained. RNA was reverse
451 transcribed using oligo dT primer and Superscript II reverse transcriptase (ThermoFisher)
452 according to manufacturer's instructions. Quantitative real time PCR was used to analyse
453 expression of *TaVIT2* and the housekeeping gene (*HKG*) *Traes_4AL_8CEA69D2F*, chosen
454 because it was shown to be the most stable gene expression across grain development in over

455 400 RNAseq samples (Borrill et al., 2016), using primer pairs qRT-*TaVIT2*-F, qRT-*TaVIT2*-R
456 and qRT-*HKG*-F, qRT-*HKG*-R, respectively. Samples were run in a CFX96 Real-Time System
457 (Bio-Rad) with the following conditions: 3 min at 95°C, 35 cycles of (5 s at 95°C, 10 s at 62°C, 7
458 s at 72°C), melt curve of 5 s at 65°C and 5 s at 95°C. *TaVIT2* expression levels were
459 normalized to expression levels of the housekeeping gene and expressed as $2^{-\Delta Ct}$.

460

461 **Perls' Prussian Blue staining**

462 Mature grains were dissected using a platinum-coated scalpel and stained for 45 mins in Perls'
463 Prussian blue staining solution (2% (w/v) potassium hexacyanoferrate (II); 2% (v/v) hydrochloric
464 acid), then washed twice in deionized water.

465

466 **Flour preparation, element analysis and phytate determination**

467 Barley grains were de-hulled by hand and all grains were coarsely milled using a coffee grinder
468 then ground into flour using a pestle and mortar. White flour fractions were obtained by passing
469 the material through a 150 µm nylon mesh. Flour samples were dried overnight at 55°C and
470 then digested for 1 h at 95°C in ultrapure nitric acid (55% v/v) and hydrogen peroxide (6% v/v).
471 Samples were diluted 1:11 in ultrapure water and analysed by Inductively Coupled Plasma-
472 Optical Emission Spectroscopy (Vista-pro CCD Simultaneous ICP-OES, Agilent, Santa Clara,
473 CA, USA) calibrated with standards; Zn, Fe and Mg at 0.2, 0.4, 0.6, 0.8 and 1mg/l, Mn and P at
474 1, 2, 3, 4 and 5 mg/l. Soft winter wheat flour was used as reference material (RM 8438, National
475 Institute of Standards and Technology, USA) and analysed in parallel with all experimental
476 samples. Phytate levels were determined using a phytic acid (total phosphorus) assay kit
477 (Megazyme, Bray, Ireland).

478

479 **Bioavailability assays in Caco-2 cells**

480 Caco-2 cells (HTB-37) were obtained from American Type Culture Collection (Manassas, VA,
481 USA) and cultured as previously described (Rodriguez-Ramiro et al., 2017). Wheat flour
482 samples were subjected to simulated gastrointestinal digestion as described (Glahn et al., 1998)
483 with minor modifications. One gram of flour was added to 5 mL of pH 2 buffer saline-solution
484 (140 mmol/L NaCl, 5 mmol/L KCl) followed by the addition of pepsin (0.04 g/mL). Ascorbic acid
485 was added at a molar ratio of 1:20 to ensure complete solubilisation of released iron.
486 Additionally, phytase (Megazymes, Bray, Ireland) was added to fully degrade phytate (myo-
487 inositol hexakisphosphate). Samples were incubated at 37 °C on a rolling table for 90 min. Next,
488 the pH of the samples was gradually adjusted to pH 5.5, bile (0.007 g/mL) and pancreatin
489 (0.001 g/mL) digestive enzymes were added, the pH adjusted to 7, and samples were incubated
490 for an additional hour. At the end of the simulated digestion, samples were centrifuged at 3000
491 g for 10 min, the gastrointestinal enzymes heated-inactivated at 80 °C for 10 min, centrifuged as
492 before, and the resultant supernatant was subsequently used for iron uptake experiments
493 similar to Bodnar et al. (2013) with little modifications. A volume of 0.5 mL of wheat digestate

494 was diluted in 0.5 mL of Eagle's minimum essential medium (MEM) and applied over Caco-2
495 cell monolayers grown in collagen-coated 12-well plates. Samples were incubated for 2 hour at
496 37 °C in a humidified incubator containing 5% CO₂ and 95% air. After incubation, an additional
497 0.5 mL MEM was added and cells were incubated for a further 22 hours prior to harvesting for
498 ferritin analysis. To harvest the cells, the medium was removed by aspiration, cells rinsed with
499 18 Ω MilliQ H₂O and subsequently lysed by scraping in 100 µl of Cellytic M (Sigma-Aldrich,
500 UK). Cell pellets were kept on ice for 15 min and stored at -80 °C. For analysis, samples were
501 thawed and centrifuged at 14,000 x g for 15 min. The supernatant containing the proteins was
502 used for ferritin determination using the Spectro Ferritin ELISA assay (RAMCO, USA) according
503 to the manufacturer's protocol. Ferritin concentrations were normalized to total cell protein using
504 the Pierce Protein BCA protein assay (ThermoFisher Scientific, UK).
505 All experiments were performed using the following controls: a) a blank digestion without any
506 wheat sample or added iron and b) a reference digestion of 50 µM of ferrous sulphate
507 heptahydrate (FeSO₄•7H₂O) solubilized in 0.1 M HCl with 1000 µM of ascorbic acid.

508 **Statistical analysis**

509 Statistical analyses (F-test, ANOVA, Student's *t*-test, Kruskal-Wallis test, regression analysis,
510 χ^2) were performed using Microsoft Excel 2010 and Genstat 18th Edition. Unless otherwise
511 stated in the text *p*-values were obtained from Kruskal-Wallis tests with Dunnett post-hoc tests.
512 When representative images are shown, the experiment was repeated at least 3 times with
513 similar results.

514 **Acknowledgements**

515 We would like to thank James Simmonds for technical assistance; Wendy Harwood for wheat
516 transformation; Alison Huttly at Rothamsted Research for the *HMW GLU-D1-1* promoter;
517 Sylvaine Bruggraber at MRC-HNR and Graham Chilvers at UEA for element analysis; Tony
518 Miller and Dale Sanders for helpful discussions. This work was funded by HarvestPlus (J.M.C.,
519 J.B. and C.U.) and by the Biotechnology and Biological Sciences Research Council (BBSRC)
520 Institute Strategic Programme Grant BB/J004561/1 (C.U. and J.B.) and DRINC2 grant
521 BB/L025515/1 (I.R.R., S.F.T. and J.B.).

522

523 **Conflict of interest**

524 Authors declare no conflict of interest.

525

526

527

528

529

530

531

532

533 **Supporting Information**

534

535 **Figure S1** Gene models and protein sequence of wheat vacuolar iron transporters.

536 **Figure S2** *TaVIT1* complements a plasma membrane iron transport-deficient yeast mutant.

537 **Figure S3** Correlation between *HMW-TaVIT2* transgene copy number and expression of
538 *TaVIT2*.

539 **Figure S4** Ferritin formation in Caco-2 cells incubated with phytase-treated flour digestates.

540 **Figure S5** Alignment of yeast codon-optimized *TaVIT1* DNA sequence with original sequence.

541 **Table S1** Wheat *VIT* genes identified in this study.

542 **Table S2** Expression analysis of *TaVIT* genes.

543 **Table S3** Element analysis of control and *HMW-TaVIT2* wheat lines.

544 **Table S4** Heavy metals in control and *HMW-TaVIT2* wheat lines.

545 **Table S5** Architectural and yield components of control and *HMW-TaVIT2* T₀ transformants.

546 **Table S6** Architectural and yield components of T₁ plants segregating from a *TaVIT2* over-
547 expressor T₀ plant.

548 **Table S7** List of primers.

549

550

551

552 **Figure legends**

553

554 **Figure 1** The wheat genome encodes two *VIT* paralogs with different expression patterns.

555 (a) Phylogenetic tree of *VIT* genes from selected plant species: *At*, *Arabidopsis thaliana*; *Gm*,
556 *Glycine max* (soybean); *Hv*, *Hordeum vulgare* (barley); *Os*, *Oryza sativa* (rice); *Sl*, *Solanum*
557 *lycopersicum* (potato); *Ta*, *Triticum aestivum* (wheat); *Vv*, *Vitis vinifera* (grape); *Zm*, *Zea mays*
558 (maize). Numbers above or below branches represent bootstrapping values for 100 replications.
559 (b) Gene expression profiles of *TaVIT1* and *TaVIT2* homoeologs using RNA-seq data from
560 expVIP. Bars indicate mean transcripts per million (TPM) \pm SEM, full details and metadata in
561 Table S2.

562

563 **Figure 2** *TaVIT2* facilitates iron and manganese transport.

564 (a,b,c) Yeast complementation assays of *TaVIT1* and *TaVIT2* in \otimes *ccc1* (a), \otimes *pmr1* (b) and \otimes *zrc1*
565 (c) compared to yeast that is wild type (WT) for these three genes. The yeast (*Sc*) *CCC1*, *PMR1*
566 and *ZRC1* genes were used as positive controls. Cells were spotted in a 4-fold dilution series
567 and grown for 2-3 days on plates \pm 7.5 mM FeSO₄ (\otimes *ccc1*), 2 mM MnCl₂ (\otimes *pmr1*) or 5 mM
568 ZnSO₄ (\otimes *zrc1*). (d) Immunoblots of total and vacuolar protein fractions from yeast cells
569 expressing haemagglutinin (HA)-tagged *TaVIT1* or *TaVIT2*. The HA-tag did not inhibit the
570 function of *TaVIT2* as it was able to complement \otimes *ccc1* yeast (data not shown). Vhp1 was used
571 as a vacuolar marker and the absence of actin shows the purity of the vacuolar fraction.

572

573 **Figure 3** Expression of *TaVIT2* in cisgenic lines.

574 (a) Diagram of the transfer-DNA construct: LB, left border; 35S, CaMV 35S promoter; *HYG*,
575 hygromycin resistance gene; *nosT*, *nos* terminator; *HMW-GLU* prom, high molecular weight
576 glutenin-D1-1 promoter; *TaVIT2*, wheat *VIT2-D* gene; RB, right border. (b) Relative expression
577 levels of *TaVIT2* in developing grains at 10 days post anthesis as determined by quantitative
578 real-time PCR and normalized to housekeeping gene *Traes_4AL_8CEA69D2F*. Plant
579 identification numbers and copy number of the *HMW-TaVIT2* gene are given below the bars.
580 Bars indicate the mean \pm SEM of 3 independent biological replicates.

581

582 **Figure 4** Perls' Prussian Blue staining for iron in grains transformed with *HMW-TaVIT2*. Grains
583 from T₀ wheat plants were dissected longitudinally (left) or transversely (right). em, embryo; s,
584 scutellum; sdc, seed coat; es, endosperm; al, aleurone, gr, groove. The transgene copy number
585 and line number are indicated on the far left. Scale bars = 1 mm.

586

587 **Figure 5** Iron and phytate content of flour milled from *HMW-TaVIT2* wheat lines. (a) Iron
588 concentrations in white and wholemeal flour from 3 control and 6 *HMW-TaVIT2* lines. Bars
589 represent the mean of 2 technical replicates and the deviation of the mean. White flour from

590 *HMW-TaVIT2* lines has significantly more iron than control lines (n = 3-4, p<0.001; see Table
591 S3 for all data). The dotted line at 16.5 µg/g iron indicates the minimum requirement for wheat
592 flour sold in the UK. (b) Phytate content of white and wholemeal flour of control and *HMW-*
593 *TaVIT2* expressing wheat. Bars represent the mean of 2 biological replicates ± deviation of the
594 mean. (c) Molar ratio of iron:phytate in control and *HMW-TaVIT2* expressing lines. Bars
595 represent the mean of 2 biological replicates and the deviation of the mean.

596

597 **Figure 6** Growth parameters of *HMW-TaVIT2* wheat.

598 (a) Number of tillers and (b) seed output of T₀ wheat plants with indicated *HMW-TaVIT2* copy
599 numbers. Bars indicate mean ± SEM of the following numbers of biological replicates: zero gene
600 copies, n = 9; 1 gene copy, n = 10; 2 -16 gene copies, n = 9; ≥ 20 gene copies, n = 6. Further
601 details given in Table S5. Asterisk indicates significant difference from negative control (One-
602 way ANOVA with Tukey post-hoc test, * p<0.05).

603

604 **Figure 7** Endosperm-specific over-expression of *TaVIT2* in barley. The *TaVIT2-5DL* gene from
605 wheat under the control of the wheat *HMW-GLU-1D-1* promoter (see Figure 3a for full details)
606 was transformed into barley (*Hordeum vulgare* var. Golden Promise). Positive transformants
607 were selected by hygromycin. (a) Mature barley T₁ grains of a control plant and two transgenic
608 lines stained with Perls' Prussian blue staining for iron. (b) Element analysis in white and
609 wholemeal flours from a control and two *HMW-TaVIT2* over-expressing barley plants. The
610 values are the mean of 2 technical replicates.